FERMILAB-PUB-14-304-APC

Preprint typeset in JINST style - HYPER VERSION

A Fast Chopper for Medium Energy Beams

Robyn Madrak[a*] **and David Wildman**[a]

[a] *Fermi National Accelerator Laboratory,*
P. O. Box 500, Batavia, IL, USA
E-mail: madrak@fnal.gov

ABSTRACT: The key elements have been constructed for a fast chopper system capable of removing single 2.5 MeV proton bunches spaced at 325 MHz. The average chopping rate is $\sim$1 MHz. The components include a pulse delaying microstrip structure for deflecting the beam, high voltage (1.2 kV) fast (ns rise time) pulsers, and an associated wideband combiner. Various designs for the deflecting structures have been studied. Measurements of the microstrip structures' coverage factors and pulse shapes are presented.

KEYWORDS: Accelerator Subsystems and Technologies.

*Corresponding author.

Contents

1. Introduction

The key elements of a chopper system have been constructed. The system includes the deflecting microstrip structures (sometimes called "slow wave" or "meander" structures), high voltage pulsers, and wideband combiners for increasing the pulse voltage.

The goal was to use the chopper in a 60 MeV H^- linac, the High Intensity Neutrino Source (HINS). HINS was to be an R&D/test linac consisting of a 325 MHz, 2.5 MeV RFQ and both normal conducting and superconducting cavities at the same frequency. It was to serve as a demonstration of the feasibility of a high intensity 8 GeV proton source [1], which would deliver beam to the Main Injector at Fermilab. Since the operating frequency of this linac is 325 MHz, not a multiple of the Main Injector's 53 MHz, it is necessary to chop out approximately one out of every six beam bunches. This avoids beam losses due to bunches which would not be captured in a Main Injector RF bucket. The chopping would be done in the 2.5 MeV (MEBT) section of the linac, after the RFQ. Due to major changes in the design for a high intensity proton source, this linac was not constructed. Nevertheless, the chopper research is interesting and could prove useful in other applications.

The chopping scheme is illustrated in Fig. 1. For a chopper plate of length L with electric field E, and protons with momentum p and velocity β, the deflection and angle of deflection, as shown in Fig. 2, are given by

$$d[m] = \frac{EL^2}{2p\beta} \quad [10^9 Vm/(GeV/c)] \tag{1.1}$$

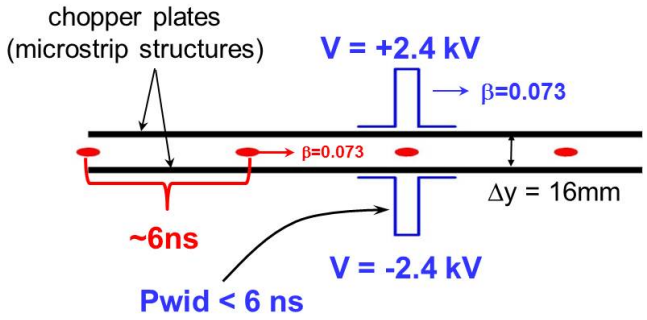

Figure 1. Illustration of the chopping scheme.

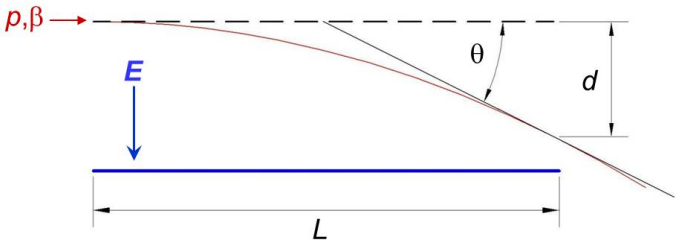

Figure 2. Deflection distance and angle by an electric field.

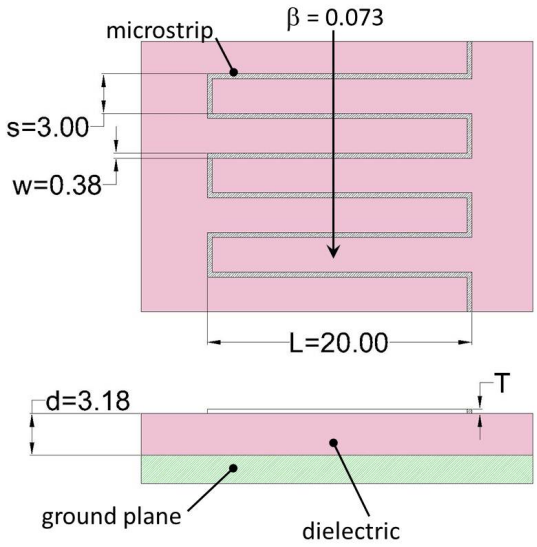

Figure 3. Views from above and end showing microstrip structure geometry.

$$\theta = tan^{-1}(EL/p\beta) \tag{1.2}$$

In order to obtain the necessary deflection, the high voltage ($\pm$2.4 kV) pulses that kick the beam propagate at the same speed as the beam (β=0.073) along two 50 cm long microstrip struc-

tures. Since the chopper must be able to remove only one bunch at a time, and the beam bunches are spaced by 3.1 ns (325 MHz bunch structure), the pulse width must be less than 6 ns. Since 325 MHz is not a multiple of 53 MHz, the chopping rate is not a single frequency. Depending on the (future) bunch position in the 53 MHz RF bucket, one or two out of every six 325 MHz bunches must be removed.

The chopper system design called for a plate spacing of 16 mm and 50 cm long deflecting structures, Due to beam dynamics constraints, and the fact that pulse dispersion is worse in longer structures, the length cannot be increased substantially. Given the size of the beam, the spacing cannot be decreased substantially. With this geometry, the required voltages are 2.4 kV on the top plate and -2.4 kV on the bottom plate. Often, the optimal solution uses deflecting structures with an impedance of 50 Ω. From an engineering perspective it was more feasible to combine the output of two 1.2 kV pulsers, each of which drives 50 Ω, with a wideband combiner. This would yield 2.4 kV driving 100 Ω. For this reason, we investigated a structures with 100 Ω impedance, and constructed combiners. The structures are discussed in Section 2. The pulsers and combiners are discussed in Sections 3 and 4.

2. Microstrip Structures

In order to slow the pulse to $\beta = 0.073$ (the speed along the beam direction), a microstrip trace pattern such as that shown in Fig. 3 can be used. The phase velocity along the microstrip is $v_p = c/\sqrt{\varepsilon_e}$, where ε_e is the effective permittivity given approximately by [2]:

$$\varepsilon_e = \left(\frac{\varepsilon_r + 1}{2}\right) + \left(\frac{\varepsilon_r - 1}{2}\right) \frac{1}{\sqrt{1 + 12d/w}} \tag{2.1}$$

where w and t are the width and thickness of the microstrip, and d and ε_r are the thickness and relative permittivity of the dielectric. For $w/d \leq 1$ the impedance is given by

$$Z_c = \frac{1}{2\pi}\sqrt{\frac{\mu_0}{\varepsilon_r \varepsilon_0}} \ln\left(\frac{8d}{w} + \frac{w}{4d}\right) \tag{2.2}$$

again, for $w/d \leq 1$.

Still, the pulse propagation velocity along the beam direction differs substantially from $v_p \times (s/(L+s))$, where L and s are the length and half period of the pattern, as shown in Fig. 3. This is due to dispersion in the periodic structure which has coupling between the adjacent microstrips. Thus, the correct parameters for the structure must be determined experimentally or with a detailed simulation.

This research began with a Z_0 = 50 Ω prototype structure for the CERN SPL[1][3]. This is double meander structure, with two 100 Ω microstrips in parallel printed onto alumina substrate ($\varepsilon = 9.8$) with thickness d = 3 mm. The microstrip width is 0.45 mm and the lateral extension of the double meander pattern is 42.5 mm (so $L = 42.5$ mm/2). Equations 2.1 and 2.2 give $\varepsilon_e = 5.9$ and $\beta \approx v_p/c \times (s/(L+s)) = 0.053$, though the actual β was known to be ≈ 0.08. The impedance is predicted fairly well by the equation, which gives 98 Ω. For a $\beta = 0.073$ structure, the CERN

[1]Many thanks to Fritz Caspers, CERN.

design was scaled (by scaling the width L of the trace pattern) to account for the difference in β of 8%. The new scaled structure is the first shown in Fig. 4. Rogers TMM10i was used instead of alumina for the new meander structure. This material also has $\varepsilon = 9.8$, however, it allows for complete prototype meanders to be made very quickly. Laminates may be procured in $18'' \times 24''$ sheets with copper cladding on one or both sides. The meander pattern can then be quickly routed out on a small programmable milling machine for PC boards which is available in-house.

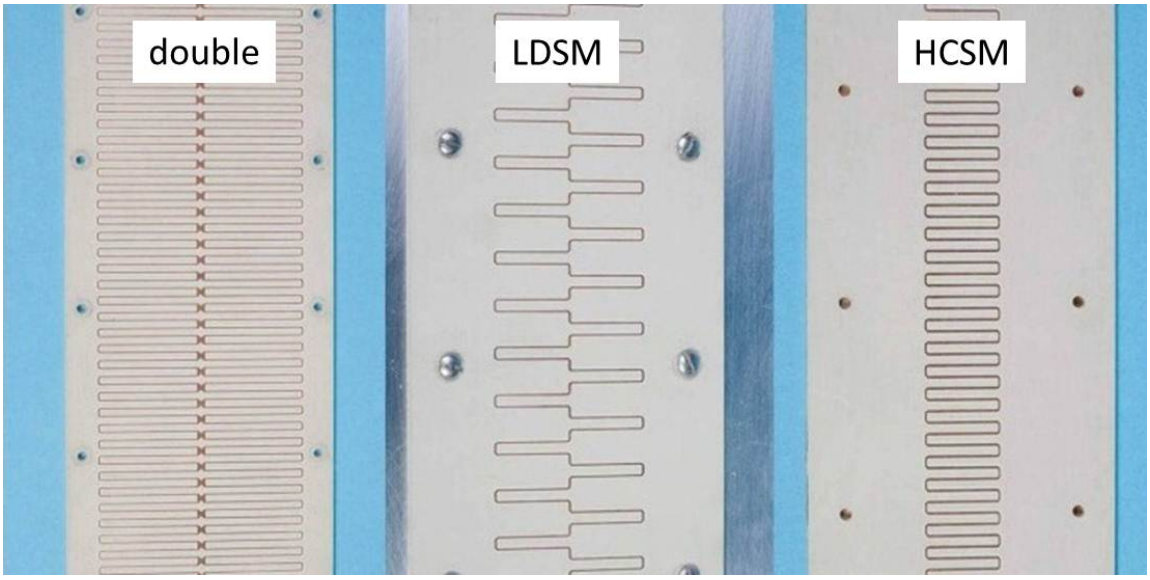

Figure 4. Three prototype microstrip deflecting structures. From left to right: the 50 Ω double meander, the 100 Ω low dispersion single meander (LDSM) and the 100 Ω high coverage factor single meander (HCSM).

Three different designs for the structure were explored. The first, already mentioned, is a 50 Ω double meander structure. The second and third have only a single trace and an impedance of 100 Ω. These are shown in Fig. 4 and are termed the "low dispersion single meander"(LDSM) and the "high coverage factor single meander"(HCSM). Each structure uses $1/8''$ thick Rogers TMM10i High Frequency Laminate Circuit Material with 70 μm Cu cladding. The prototype structures are $18''$ (46 cm) long. This is 4 cm shorter than the design for the final structure, but minimizes waste since the TMM10i is produced in sheets of $18'' \times 24''$ (46×61 cm). The transverse extent of the traces is 78 mm for the double meander, 40 mm for the LDSM and 20 mm for the HCSM. In each case the width of the trace is 0.38 mm

2.1 Pulse Dispersion Measurements

Fig. 5 shows the pulse behavior at the beginning, middle and end of the three structures. Also shown is the (low voltage) input pulse. The pulse shapes are sampled using a HP high frequency scope probe. The pulse in the double meander structure broadens substantially. Both single structures show little increase in the pulse width as it travels, though the degradation is the least in the LDSM. This is expected since the separation between the traces is the largest in this case, so there is less coupling and dispersion.

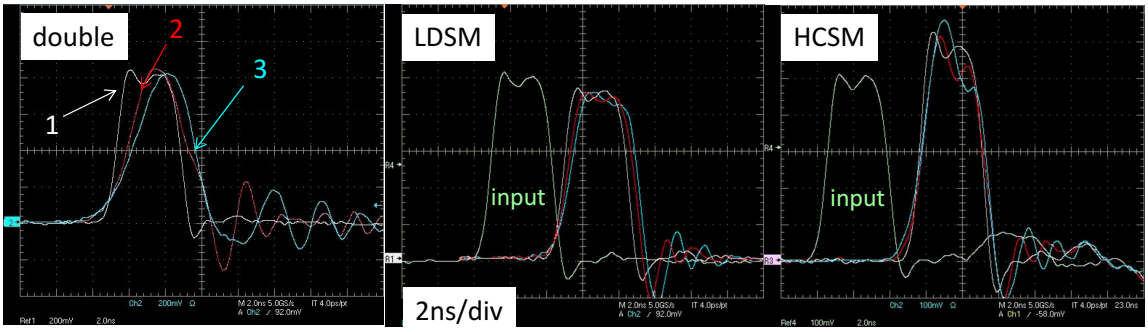

Figure 5. Three scope photos showing scope traces sampled using a high frequency probe. These show the evolution of the shapes of the pulses as they travel down the three different prototype microstrip structures. The input pulse is the leftmost pulse shown for the LDSM and the HCSM. On the scope photo for the double microstrip structure, the pulses are color coded and indicated with arrows at the beginning (1), middle (2), and end (3) of the microstrip structures. The color mapping and order is the same for the other two scope photos. Note that in all three cases, the peak voltage of the input pulse is different, but the shape is the same. Also the scale in mV/div is not the same for the input pulse as it is for the output pulses, and is not the same in all three photos.

2.2 Coverage Factor

Since the metal traces of the microstrip structure are not solid conductor, the effective electric field seen by the beam is less than the voltage difference between the pulses on the two structures divided by their separation. The leads to the definition of the coverage factor:

$$C = \frac{E}{\Delta V / \Delta y} \tag{2.3}$$

where E is the actual electric field between the plates seen by the beam, ΔV is the voltage difference between the pulses on the upper and lower structures, and Δy is the plate separation. Generally, the smaller the fraction of conducting area, the smaller the coverage factor.

The coverage factor as a function of transverse position has been measured for each structure, using the fixture shown in Fig. 6, along with a network analyzer. This is a transmission S_{21} measurement with the input signal (Port 1) connected to the microstrip trace and the transmitted signal (Port 2) connected to a HP85024A high frequency probe which serves as a pickup. The probe tip is placed the same distance away from the surface as the beam would be ($y = 8$ mm) and is surrounded by a ground plane which is electrically connected to the microstrip structure ground plane. This ground plane at the vertical position of the beam replaces a virtual ground which would be present in the real chopper system when the upper structure is placed above (and as a mirror image of) the lower structure. The probe is mounted on micrometer adjustable stages so that it may be moved in the x and z directions. The z direction is parallel to the beam direction and x is perpendicular to both beam direction and to the vertical as shown in Fig. 6. For normalization, a wide (25 mm) stripline is used. In this case, the probe tip is located at one of the stripline ground planes. Each ground plane is 8 mm from the stripline center conductor. Measurements of the 100 Ω structures are corrected for reflection due to the impedance mismatch between the network analyzer (50 Ω) and the structure. The coverage factor measurements at the center of the microstrip structures (x=0) are shown

structure	coverage factor
double	71%
LDSM	48%
HCSM	74%

Table 1. Measured coverage factors at the center for the three prototypes.

in Table 1. Approximately 50% higher voltage would be needed to obtain the same deflection from the LDSM as from the HCSM. The coverage factor for the 50 Ω structure is larger, though twice as much power per pulse is needed to drive the smaller impedance to the same voltage. Fig. 7 shows measurements of the coverage factor versus transverse position on the meander. Given that the dispersion in the HCSM is acceptable, and the fact that it has a much higher coverage factor than the LDSM, the HCSM is a good compromise.

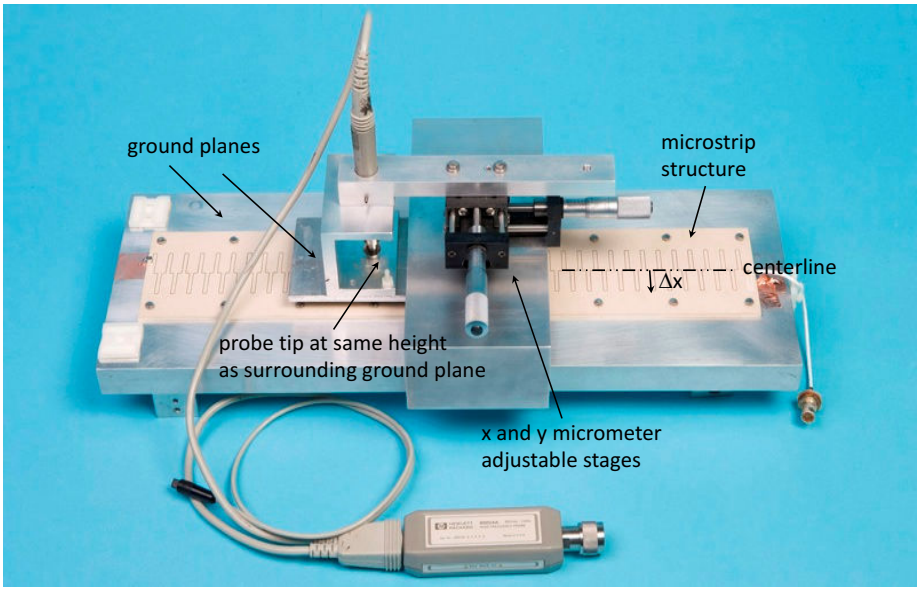

Figure 6. Fixture used with network analyzer for measurement of coverage factor.

2.3 Vacuum Compatibility

To test for suitable behavior of Rogers TMM10i in vacuum, a 24×13 cm sample was baked for 90 hours at 170 °C. The pressure and temperature during the bakeout are shown in Fig. 8. After the bakeout the pressure was 8×10^{-8} torr at 55 C (the predicted operating temperature of the structure, given losses) with a relatively low pumping speed of 0.63 L/s. Given that the surface area of the sample is a factor of three lower than that of the two structures which would comprise the final chopper, vacuum levels on the order of 10^{-8} torr should be obtainable (using a larger vacuum pump) without much difficulty. Though the vacuum properties appear acceptable, the sample was discolored after the bake. In addition, the radiation resistance was not studied. Without further

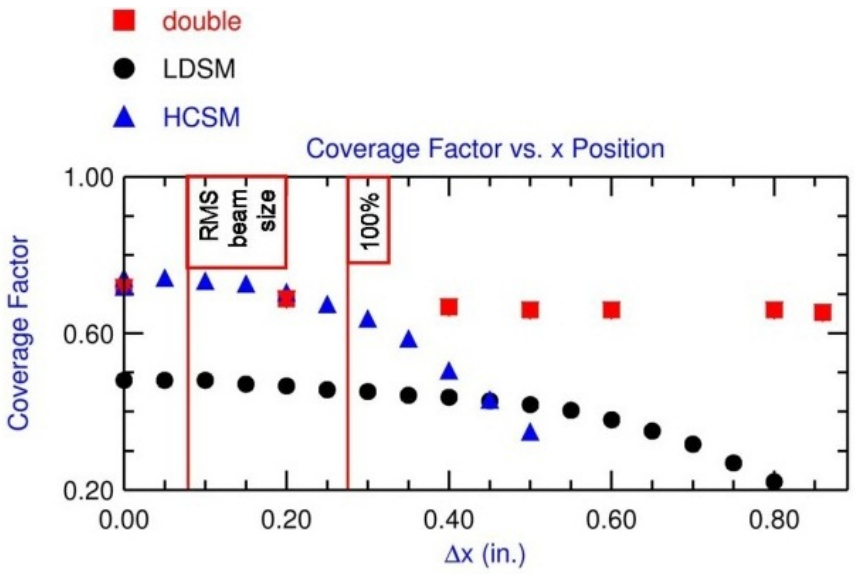

Figure 7. Measured coverage factor as a function of distance from the center of the structure, for the three prototype structures.

measurements conservatism might dictate the use of alumina as opposed to the composite material. Nevertheless it is very useful at the R&D stage for fast and economic prototyping.

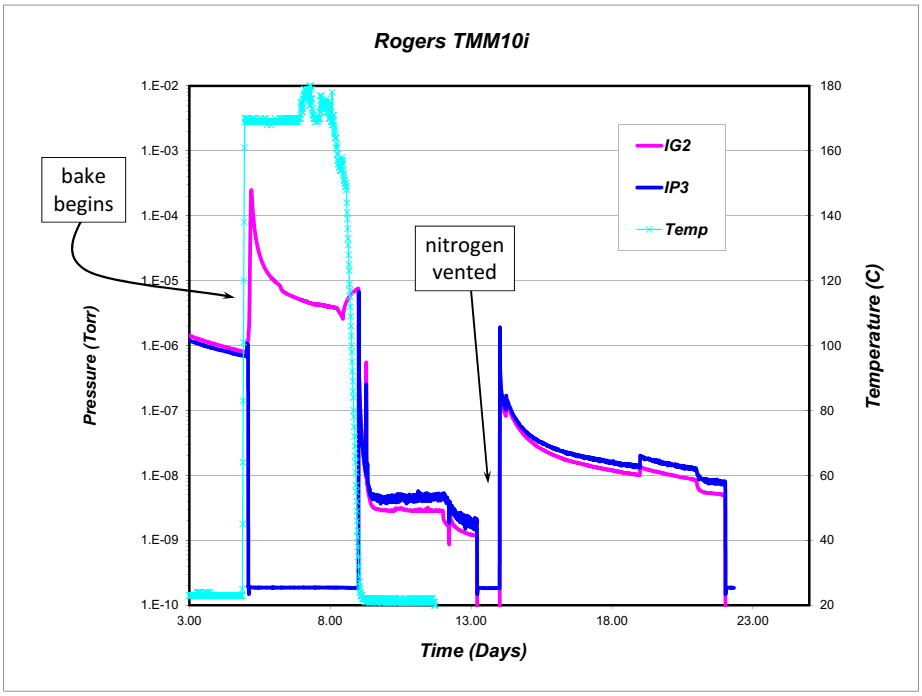

Figure 8. Pressure (IG2 and IP3, left axis) and temperature (right axis) during the bakeout of Rogers TMM10i, with a 0.63 L/s ion pump. After ∼13 days, the vacuum vessel containing the sample was vented with nitrogen for 4 hours. After the vent, pumping was continued.

3. Fast High Voltage Pulser

Fermilab has first procured from Kentech Instruments, Ltd. a prototype 500 V pulser, and later, a 1.2 kV pulser. The 1.2 kV is the final version of the pulser and a total of four are needed for the entire system. The average chopping rate imposed by the beam pulse parameters (1 ms pulses at 10 Hz or 3 ms pulses at 2.5 Hz) is close to 1 MHz. The switching losses in high voltage (kilovolt) semiconductor switching devices becomes excessive at these pulse rates. In order to obtain fast rise and fall times, together with a high pulse repetition rate, the output is generated from an array of custom packaged low voltage (100 V) semiconductor switches. These relatively low voltage parts have a bandwidth of ∼500 MHz allowing nanosecond rise and fall times. The pulser may be operated in 1 ms mode or 3 ms mode. The maximum total on-time during a 1 ms burst is 0.75 ms. Fig. 9 shows the pulser output (attenuated by 60 dB). The top scope photo shows several 1.2 kV pulses spaced by 20 ns. The bottom shows a full 3 ms burst of this pulse pattern.

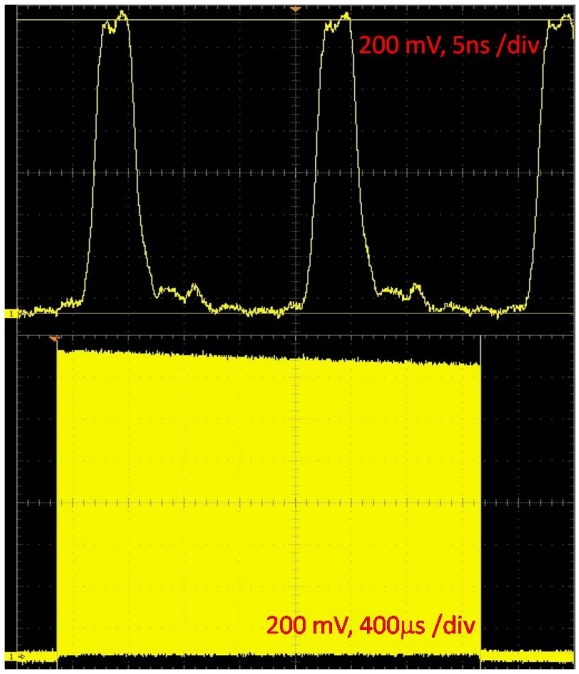

Figure 9. Pulser output attenuated by 60 dB, on oscilloscope. The top trace (5 ns/div) shows several single 1.2 kV pulses. The bottom trace (400 μs/div) shows a full 3 ms burst.

4. Wideband Combiner and High Voltage Pulses on Structure

Two combiners (coaxial cable impedance transformers) were built to combine the 50 Ω outputs of high voltage pulsers. In the initial chopping scheme, one combiner would combine the outputs of two 1.2 kV pulsers for the bottom structure, and one combiner would combine the outputs of two -1.2 kV pulsers for the top structure. The combiner idea is illustrated in Fig. 10. The inner conductor of the first 50 Ω cable is connected to the outer conductor on the second 50 Ω cable. The inductance due to cable wound on the the ferrite presents a large impedance to pulses from

source 1 from to ground on source 2. Each combiner was built using 46 turns of Andrew FSJ2-50, $\frac{3}{8}''$ heliax ® superflexible foam coaxial cable, wrapped around five $1''$ thick ferrite cores. The core material is MN60 with an OD and ID of $11''$ and $4.5''$. A photograph is shown in Fig. 11.

The number of cores used was optimized by calculating the total number of turns (n) that could be made as a function of number of cores (N) for a given length of cable. (As the number of cores increases, the length per turn increases). The given length was chosen to be 1055 inches. This was chosen since it would be the resulting length in a perfectly wound combiner with 2 cores, if the space inside of the ID of the cores was completely filled. In addition, the losses were also acceptable for this length of cable. Inductance, which is proportional to $N \times n^2$ is a maximum for $N = 5$, so five cores were used.

For a pulse of length t (maximum 3 ms in this case) the voltage across the inductor is

$$V = V_0(1 - \alpha l)\exp(tR/L) \tag{4.1}$$

Where V_0 is the initial voltage, α is the loss per length of cable, l is the length of the cable and is a function of n, R is the resistance (50 Ω in this case) and L is the inductance, also a function of n. Once the optimal number of cores was known, the optimal number of turns n was calculated by noting the maximum of Eq 4.1 as function of n. The optimal value in this case was 51. Theoretically it should have been possible to wind 51 turns on 5 cores, but in reality is was only possible to fit 46 turns.

One nearly[2] complete system has been tested. The outputs of two pulsers – one 0.5 kV and one 1.2 kV – were combined using the wideband combiner. The pulses were propagated down the meander structure, which was terminated into a low inductance 100 Ω resistor. A high frequency scope probe was used to view the pulses at the resistor, and are shown in Fig. 12. The output pulses have a maximum voltage of approximately 1.6 kV and are slightly dispersed compared to the original pulser output, however, the time between rise from 5% maximum voltage and fall to 10% maximum voltage is still ≈ 5 ns.

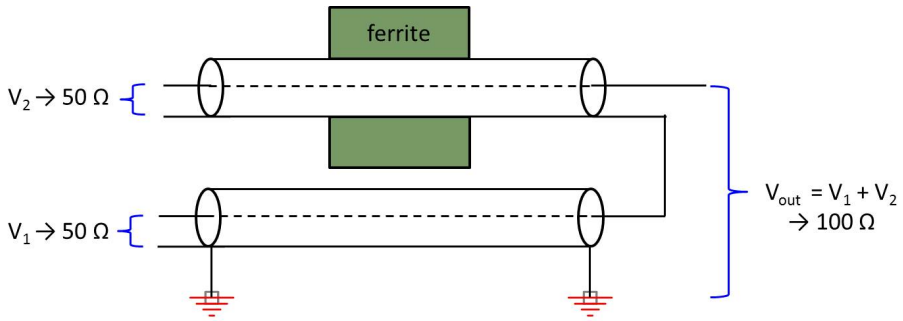

Figure 10. Combining of two 50 Ω outputs to one 100 Ω output.

[2] a truly complete system would use two 1.2 kV pulsers, but only one 1.2 kV and one 0.5 kV pulser had been fabricated and purchased.

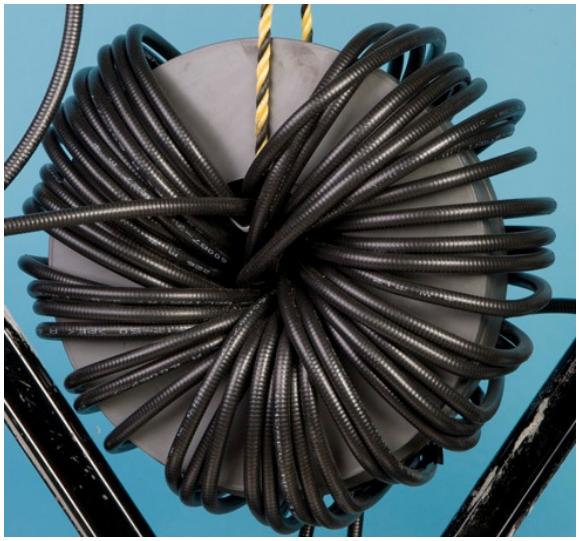

Figure 11. One combiner with $\frac{3}{8}''$ Heliax superflexible cable and five $1''$ thick MN60 ferrite cores.

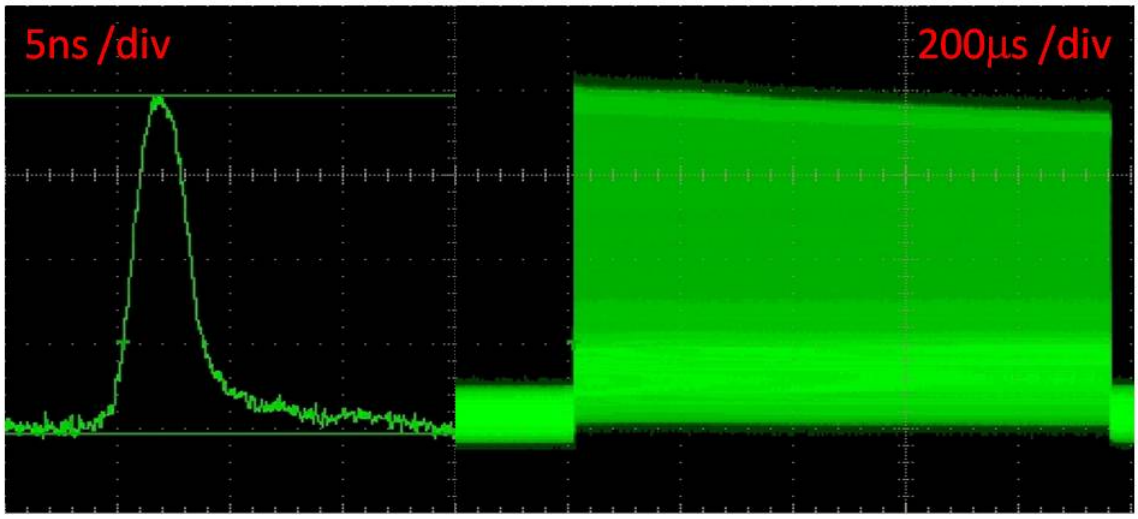

Figure 12. Combined output pulses from 0.5 and 1.2 kV pulses, after traveling down the prototype microstrip structure. The output pulses are ≈1.6 kV and are viewed using a scope probe on a 100 Ω low inductance resistors which terminates the structure.

5. Summary

Various components needed for a chopper system for pulsed 2.5 MeV proton beam have been constructed. Several patterns for deflecting microstrip structures have been studied. A high voltage pulser with the necessary pulse width and voltage has been procured, though a total of four are needed for the full system. A wideband combiner for obtaining the necessary voltage on the structures, by summing the outputs of two pulsers, has been built. All of the available components have been tested together, and the results are promising.

The initial motivation for these studies was the design of a chopper for use in a pulsed 8 GeV

high intensity proton linac. There are no near-term plans to build this machine, however, the studies and concepts here could be useful for other chopper systems.

6. Acknowledgments

We wish to thank F. Caspers (CERN) for many useful discussions and for providing the double meander structure with which we began our studies. We also wish to thank Terry Anderson (FNAL) for performing the TMM10i vacuum test.

References

[1] P. Ostroumov, Physics design of the 8 GeV H– Linac, New J. Phys. 8 (2006) 281.

[2] D. Pozar, Microwave Engineering, Third Edition, John Wiley and Sons, Inc., 2005.

[3] F. Caspers, et al., Fast chopper structure for the cern superconducting proton linac, in: Proc. EPAC 2002, Paris, 2002, pp. 873–875.